Cardiovascular Pathology 38 (2019) 31–38

Contents lists available at ScienceDirect

Cardiovascular Pathology

Original Article

# Morphology and mechanisms of a novel absorbable polymeric conduit in the pulmonary circulation of sheep☆

Marieke Brugmans [a], Aurélie Serrero [a], Martijn Cox [a], Oleg Svanidze [b], Frederick J. Schoen [c,*]

[a] Xeltis BV, De Lismortel 31, 5612AR, Eindhoven, The Netherlands
[b] Xeltis AG, Muhlebachstrasse 28, Zurich, Switzerland
[c] Department of Pathology, Brigham and Women's Hospital and Harvard Medical School, 75 Francis Street, Boston, MA, USA

ARTICLE INFO

*Article history:*
Received 1 August 2018
Received in revised form 18 October 2018
Accepted 19 October 2018

*Keywords:*
Tissue engineering
Endogenous tissue restoration
Absorbable polymer
Pulmonary artery graft
Arterial remodeling

ABSTRACT

*Background:* Right ventricular outflow tract (RVOT) conduits used in children with congenital heart disease often degenerate rapidly or develop other complications, and they do not grow with the patient. This leads to multiple surgeries until adult-sized conduits can be implanted. We report experimental in vivo experience with an entirely synthetic absorbable graft, designed to be replaced by tissue in-vivo by host cells, in a process termed Endogenous Tissue Restoration (ETR), and to grow commensurate with somatic growth.
*Methods:* We characterized the structure, mechanical properties, biocompatibility, and in vivo remodelling of a bioabsorbable polyester based on the self-complementary ureido-pyrimidinone (UPy) quadruple hydrogen-bonding motif. Electrospinning was used to process the polymer into a tubular graft with a highly porous wall structure, which was implanted as a pulmonary artery interposition graft in 9 adult sheep with a maximum follow-up of 1 year, followed by pathologic and mechanical analysis.
*Results:* All grafts were patent by transthoracic echocardiography. Eight were intact at post-mortem examination. One graft had aneurysmal dilation. Graft polymer resorption in vivo was consistent among specimens. Histologic examination revealed progressive tissue replacement of graft polymer, ongoing at one year, with remodeling to a structure that had some key features of native vascular wall. Burst pressures for all explants at 8 weeks and beyond were higher than those of native pulmonary artery (PA) and largely determined by newly formed tissue.
*Conclusions:* Preclinical studies of a new, absorbable polymeric graft for PA replacement showed remodelling by endogenous cells up to one-year follow-up. Our results show that ETR leads to progressive and substantial replacement of an off-the-shelf synthetic bioabsorbable conduit by functional host tissue to one year in sheep. Thus, further development of this novel concept is warranted.



## 1. Introduction

Approximately 100,000 infants are born worldwide each year with life-threatening complex congenital defects affecting the heart chambers, great vessels and valves [1]. The standard of care in cardiac surgery to repair complex congenital malformations typically uses synthetic grafts, homografts or xenograft tissue in the right ventricular outflow tract. However, this strategy may be associated with complications including tissue overgrowth, thromboembolism, infection, calcific and mechanical degradation, and possibly rejection [2–4]. In addition, since contemporary grafts are unable to enlarge to accommodate maturation and growth of a young recipient, many such children require multiple surgeries to replace conduits that have become complicated or degenerated or insufficient owing to somatic growth of the patient [5].

To overcome these limitations, investigators have been working on several distinct regenerative approaches to yield a graft composed of healthy living tissue that could potentially grow. The *in vitro* tissue engineering approach uses cells seeded on an absorbable polymeric scaffold, cultured in a bioreactor (typically for several weeks and often with cyclic mechanical loading) to form a composite of polymer and new tissue (a *construct*), which becomes the implant [6–9]. A different approach utilizes intraoperatively stem cell-seeded bioabsorbable polymer implants in a vascular configuration, bypassing the bioreactor phase. This concept was brought to clinical application as a Fontan conduit [10]. Other investigators have either incorporated bioactive factors into a synthetic absorbable implant, or generated de-novo tissue in vitro for direct implantation [11], thereby avoiding the complexities

*Abbreviations:* ETR, Endogenous tissue restoration; H&E, Hematoxylin and eosin; RVOT, Right ventricular outflow tract; UPy, Ureido-pyrimidinone.

☆ Disclosure: Frederick J. Schoen is a member of the Scientific Advisory Board of and a consultant to Xeltis BV. Dr. Schoen also is consultant to LivaNova, Medtronic, Neograft Medical and TissX.

* Corresponding author.
*E-mail address:* fschoen@bwh.harvard.edu (F.J. Schoen).

https://doi.org/10.1016/j.carpath.2018.10.008
1054-8807/

associated with the use of stem cells [12]. Advances in materials research and development have permitted the possibility of an alternative strategy — a regenerative graft fabricated solely from and implanted as a bioabsorbable polymer matrix designed to remodel in-vivo to yield a fully functioning blood vessel composed of healthy native autologous tissue. The formation of living tissue would be mediated entirely by cells of the recipient, without the use of (exogenous/manipulated) stem cells, added bioactive factors, or other animal-derived products. This strategy has been termed In-Situ Tissue Engineering or Endogenous Tissue Restoration (ETR) [13–16]. The latter term will be used in the present discussion.

The preclinical study in adult sheep reported herein used a vascular graft, composed of a bioabsorbable supramolecular polyester, based on the 2-ureido-4[1H]-pyrimidinone (UPy) motif, that is designed to enable ETR [17]. This class of materials has several advantages. First the supramolecular bonds make the polymer chains self-organize into nanostructures, which increase mechanical strength and chemical stability. As a consequence, similar properties to those of conventional polyesters can be achieved at much lower molecular weights by viscosity-depended manufacturing techniques such as electrospinning. Secondly, the supramolecular nature of the polymer facilitates controlled alteration of mechanical properties and absorption rates and potentially biological responses throughout a broad range by altering the polymer chemistry (e.g., through interchanging backbones and ratios between compounds) [18].

In this sheep animal model study, extending to one year, we focused on the interactions of the bioabsorbable polymeric vascular graft biomaterial with the surrounding tissue during ETR. including absorption and tissue formation.

## 2. Materials and methods

Preclinical investigations were performed using a new vascular graft (Xeltis BV, Eindhoven, The Netherlands), fabricated as a sterile, straight, polyester conduit, and processed by electrospinning. The polyester is obtained by chain-extending poly-caprolactone with the supramolecular UPy-motif. The graft matrix is flexible, porous and designed to allow endogenous cell penetration and subsequent tissue growth without the added administration of stem cells, growth factors or other biological products. Fig. 1 shows a scanning electron photomicrograph of the graft.

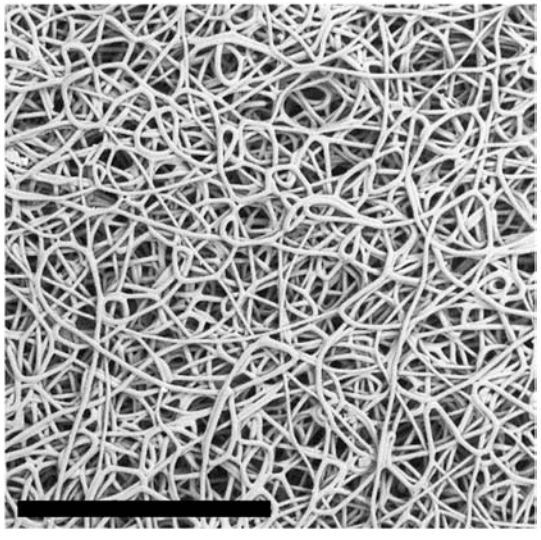

**Fig. 1.** Wall microstructure of polymeric pulmonary arterial conduit. Scanning electron photomicrograph. Bar = 250 um.

### 2.1. Preclinical animal investigation: surgery, performance evaluation and explantation

Nine adult sheep (weight range 46–78 kg) received the vascular conduit in the pulmonary artery, with different follow-up intervals. All implants were of 20.8mm inner diameter as measured by caliper, and a wall thickness of 1.0mm as measured by laser. Implants were cut to length 35+/-4mm during the procedure. All animals were operated in a dedicated animal facility, under general anesthesia and normothermic cardiopulmonary bypass on the beating heart. One animal was sacrificed after 5 days to evaluate the early histologic response to the graft. Other implants were followed up for 8 to 53 weeks (See Table 1).

Under general anesthesia, a muscle sparing left anterolateral incision was performed and the chest entered in the third intercostal space. After opening the pericardium, the main pulmonary artery was exposed. Heparinization was achieved by an intravenous injection of 100 U/kg of Heparin and repeated to maintain the activated clotting time over 300 s. Under cardiopulmonary bypass, the pulmonary artery was transected above the pulmonary valve and the conduit was implanted as an interposition graft with two end-to-end anastomoses using running sutures (Fig. 2). Postoperative anticoagulation was performed with 20 mg bid of Enoxaparin for 5 days. For animals in the 8 week study, antibiotic treatment consisted of Cephamandole at the dose of 20 mg/kg/IV or IM 2×24 h for 2 days and IM for 6 days. Anticoagulation and anti-aggregation treatment consisted of Calciparin 0.8ml/SC/2×24 h/90 days and aspirin 250 mg/SC/day until sacrifice. For all other animals, antibiotic treatment consisted of Ceftiofur 2.2 mg/kg IM for 5 days, and anticoagulation with Enoxaparine 40 mg SID for 5 days and then 40 mg/SC/1×24 h/90 days, and Aspirin 250 mg/SC/day/until sacrifice.

Hemodynamic and morphologic assessment was performed at 8 weeks and later in a monthly interval by transthoracic echocardiography; the diameter and patency of the implanted grafts were analyzed at the level of the proximal and distal anastomosis and at the middle of the conduit. The postoperative course was assessed for adverse events and animals were sacrificed at the predetermined time points following surgery. A full post mortem examination was performed on all sheep following sacrifice. Explanted vascular grafts were analyzed for mechanical strength and histology. Explanted conduits were cut into 5 mm cross sections for mechanical tests (native tissue and at different locations of the graft) or histology (mid- graft).

### 2.2. Mechanical testing

Uniaxial tensile tests were performed on bare scaffolds and unfixed strips cut from all explanted grafts at 8 weeks and beyond. Strips were cut to 5 x 25mm and elongated until break at a speed of 10 mm/min using a Multitest 1-I with a 50N load cell (Mecmesin, UK). Ultimate Tensile Strength (UTS) was used to calculate a derived burst pressure based on Laplace's law. To evaluate the mechanical properties of the remaining polymeric scaffold, tissue was removed by treating the explants

**Table 1**
Overview of implants and follow-up

| Ovine | Age at implant (years/months) | Weight at implant | Pre-op echo native PA diameter | Follow up time |
|---|---|---|---|---|
| #1 | 1y 9m | 60 kg | ND | 5 days |
| #2 | 1y 4m | 46 kg | 1.75cm | 8 weeks |
| #3 | 1y 2m | 51 kg | 2.0cm | 8 weeks |
| #4 | 3y 2m | 78 kg | 2.3cm | 10 weeks |
| #5 | 3y 2m | 59.5 kg | 2.1cm | 11 weeks |
| #6 | 2y 11m | 73 kg | 2.4cm | 24 weeks |
| #7 | 3y 2m | 68.5 kg | 2.1cm | 40 weeks |
| #8 | 3y 2m | 66.5 kg | 2.1cm | 53 weeks |
| #9 | 2y 11m | 74.5 kg | 2.0cm | 53 weeks |

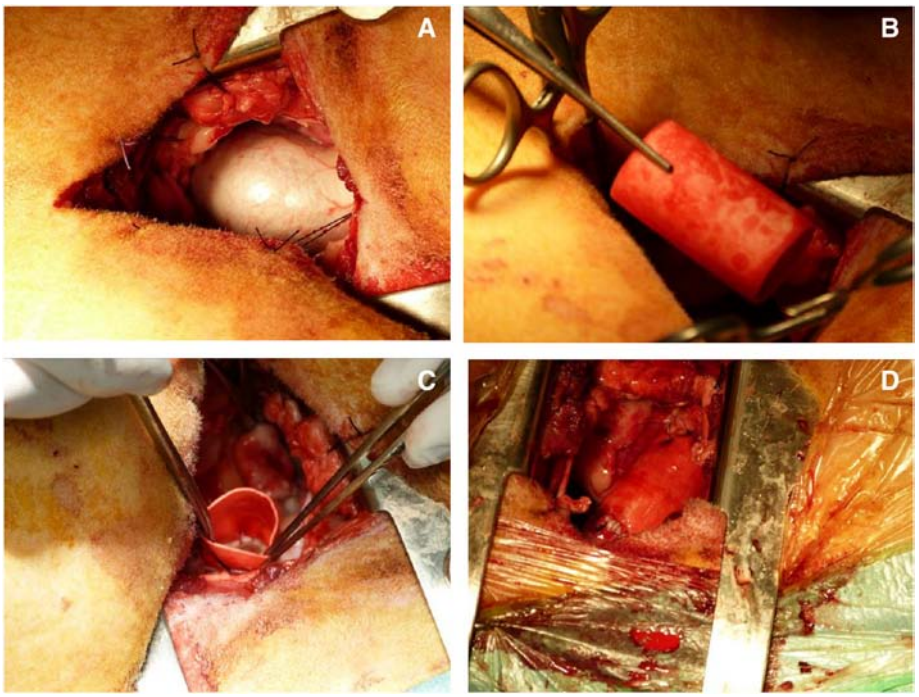


**Fig. 2.** Surgical implantation of the vascular graft. (A) native pulmonary artery; (B) pre-clotted graft; (C) suturing the vascular graft on the native artery; and (D) the implanted vascular graft.

with 10 ml Clorox® [19]. As a control, native ovine pulmonary arteries were obtained during the implantation procedure and tested in a fresh condition similarly to the explant material.

### 2.3. Pathological evaluation

Gross pathologic examination and conventional histological analysis following fixation in 3.7% formaldehyde were done. Staining of histologic sections included: H&E (hematoxylin-eosin) for evaluation of tissue morphology; Masson's Trichrome for evaluation of collagen and Von Kossa for evaluation of calcium phosphates. In addition, special immunohistochemical stains were performed: Von Willebrand Factor for evaluation of neovascularization and endothelialization; Smooth Muscle Actin to identify smooth muscle cells and myofibroblasts; CD 45 for evaluation of leukocytes and Van Gieson staining for elastin and evaluation of connective tissues. Semi-quantitative evaluation of polymer absorption and collagen deposition was performed by CV Path Institute, Gaithersburg, USA. The histologic grading system is described in Table 2.

**Table 2**
Description of semi-quantitative scoring for scaffold absorption and collagen deposition

| Attribute | Score | Description of Assigned Score |
|---|---|---|
| Scaffold absorption score | 0 | No absorption of scaffold |
| | 1 | < 10% conduit shows scaffold absorption |
| | 2 | 10-<25% conduit shows scaffold absorption |
| | 3 | 25-<50% conduit shows scaffold absorption |
| | 4 | 50-<75% conduit shows scaffold absorption |
| | 5 | >75% leaflet conduit shows scaffold absorption |
| Collagen deposition | 0 | No collagen deposition |
| | 1 | Collagen deposition <10% |
| | 2 | Collagen deposition 10-<25% |
| | 3 | Collagen deposition 25%-<50% |
| | 4 | Collagen deposition 50%-<75% |

## 3. Results

### 3.1. In-vivo animal model

All animals survived the surgical procedure. Post-intubation tracheitis occurred in two animals at 2 and 4 weeks after the operation, respectively, and both cases were resolved with antibiotic therapy. Echocardiographic follow-up was done in the eight longer-term animals. All grafts remained patent, without evidence of stenosis. The evolution of mid-graft diameter during the study period is shown in Fig. 3. Compared to the mean diameter of the native main pulmonary artery of 21±2 mm at pre-operative echocardiography, evaluation at follow-up showed no significant changes in graft diameter in 7 of 8 chronic animals. However, one animal sacrificed 10 weeks after implantation (number 4), had a 49 mm fusiform aneurysmal dilation in the mid-section of the graft which had been initially noted at 8 weeks echocardiography.

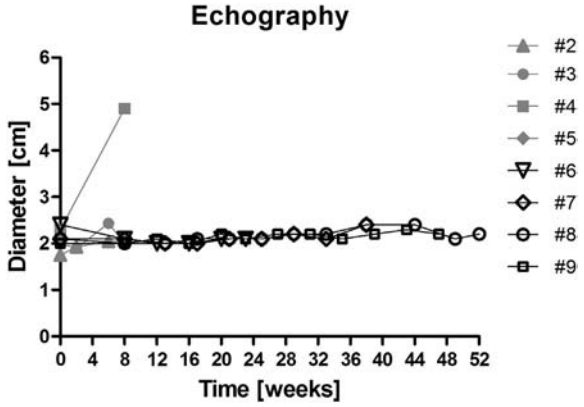


**Fig. 3.** Progression of mid-graft diameter, measured via echocardiography during follow up period. T=0 is the diameter of the native artery. Each line indicates a different animal. Graft in animal #4 had aneurysmal dilation.

All animals appeared healthy at the end of the study period. However, some animals had uncomplicated pericardial and pleural adhesions, which were attributable to the implantation and not graft-related.

### 3.2. Mechanical strength

The derived burst pressures at all time points were well above the required safety limits of 120 mmHg (a very severe right ventricle peak systolic pressure), based on ISO5840-3:2011 and higher than the native pulmonary artery (620 mmHg) and the unimplanted scaffold (796 mmHg) as shown in Fig. 4. Burst pressure in the aneurysmal region observed in one graft was 1352 mmHg. The burst pressure of the remaining scaffold (with tissue removed) was lower than the burst pressure of the explant at 8 and 11 weeks and was not measurable at 10, 24, 40 and 53 weeks follow-up.

### 3.3. Histology

Histological evolution of grafts to 53 weeks demonstrated progressive changes beginning with host cell infiltration to extensive polymeric graft absorption and replacement by tissue and luminal coverage by neointima. Leukocyte infiltration was observed in all grafts, highlighted by CD45 staining. At 5 days following implantation, the graft was intact and there was minimal detectable influx of inflammatory cells (data not shown). Subsequently, as summarized in Figs. 5-9, all grafts showed extensive inflammation with phagocytosis of the polymeric graft fibers, in a typical foreign body response containing abundant giant cells. There was progressive resorption of the polymer matrix and its replacement by collagen at extended implantations times with increasingly broad fascicles separating areas of active graft resorption and ingrowth of blood vessels from surrounding tissues. In grafts with the longest follow-up, there was more collagen and lesser ongoing phagocytic activity, with reduced inflammatory infiltrate. Extensive scaffold fragmentation was demonstrated after 24 weeks (as noted in Fig. 8), and less scaffold fragments remained in the explants at 38 and 53 weeks. At 53 weeks, islands of residual graft material were embedded in distinct transmural bands of vascularized fibrous tissue and the macrophage activity was focused on removal of the remaining scaffold particles (as noted in Fig. 9A). While the fibrous bands separating areas of residual polymeric graft were largely devoid of smooth muscle cells, the luminal surface was covered with fibrous tissue composed of smooth muscle cells and collagen (as noted in Fig. 9B and C, respectively). This layer was partially lined by a single cell layer that resembled endothelium and stained for von Willebrand Factor (as noted in Fig. 9E). At no site was there evidence of peeling of the neointima from the inside surface of the graft wall. No calcification of the grafts was noted. Portions of some of the longer-term grafts showed focal deposition of bandlike elastin at the junction of the neointima with the underlying, remodeling graft wall, and additional elastin fragments in the neointima (as noted in Fig. 9D).

Semi-quantitative analysis of the histological pictures shows that the absorption scores increase over time simultaneously to increased collagen deposition score (see Table 3 and Fig. 10). The graft with aneurysmal dilation (#4) is an exception, where both the absorption and collagen deposition scores are 3 (i.e., relatively high).

## 4. Discussion

The studies described above provide evidence for the in vivo structural evolution and intermediate-term functionality of an electrospun, bioabsorbable polyester vascular graft implanted as an interposition conduit in the pulmonary artery in sheep with a follow-up to 12 months. The surgical procedure to implant the graft was feasible and safe. There were neither serious adverse events nor graft-related complications in 8 out of 9 sheep and no incidence of structural deterioration, malfunction or stenosis in grafts or their anastomoses. Echocardiography throughout the follow-up period confirmed good functionality and hemodynamic performance of all but one graft discussed in detail below.

Mechanical testing of the explanted grafts (as composites of polymer and new tissue) demonstrated that the derived burst pressure at all intervals of follow-up was of an order of magnitude higher than the safety limit of 120 mmHg, with an average burst pressure of 1355 mmHg for the explants after 8 weeks and later. Since the burst pressure of the bare scaffold (tested pre-implantation) was 796 mmHg, the new tissue contributes significantly to graft functionality. The burst pressures of the remaining scaffold determined at 8 and 11 weeks (tested following post-explanation tissue removal) were much lower than the burst pressure of the explants, showing a decreasing contribution of the scaffold to the overall graft strength as new tissue assumes a greater portion of the load. After 11 weeks, the strength of the remaining scaffold was too low to measure.

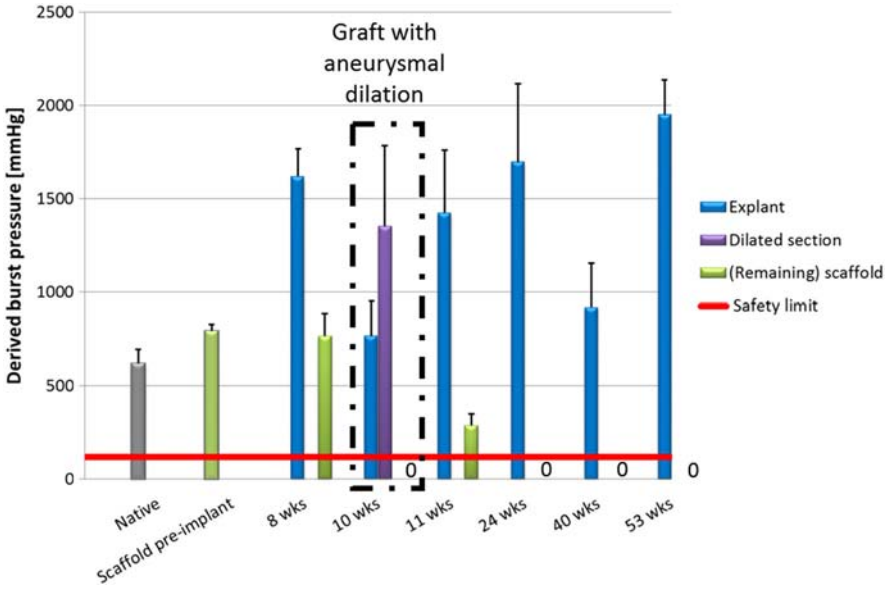


**Fig. 4.** Derived burst pressures of explants at different times. Bare scaffold and native ovine pulmonary artery burst pressures are provided as controls. The safety limit of 120 mmHg based on ISO5840-3:2011 is indicated in red. Note that two animals are combined at 8 weeks and 53 weeks.

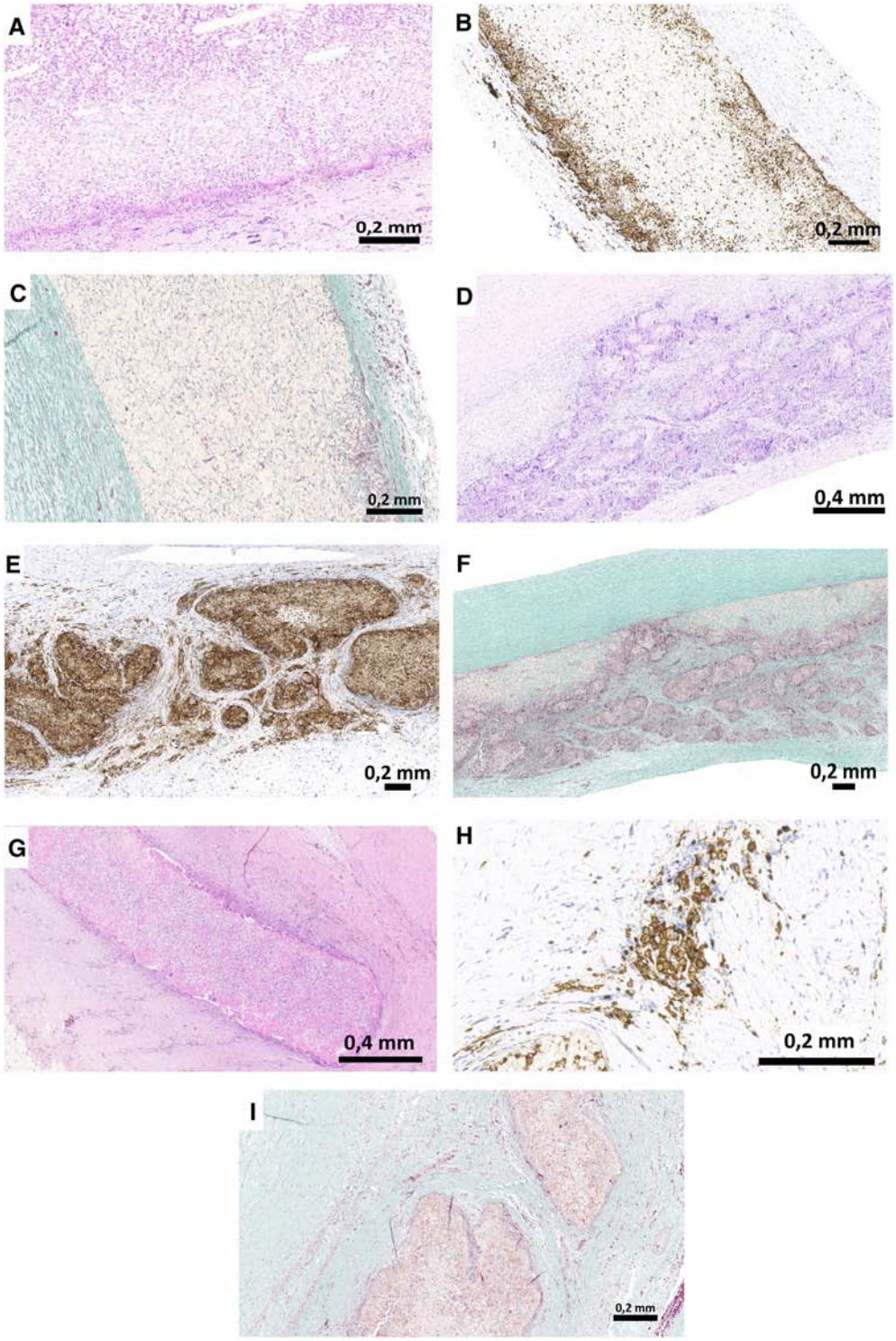


**Fig. 5.** Photo composite showing progressive absorption of polymeric graft material and replacement by host tissue over 8-53 weeks. At 8 weeks post-implantation (A, B and C) the graft configuration is intact, with recipient inflammatory cells infiltrating the graft diffusely from the luminal and external surfaces; no collagen is yet present within the graft. At 24 weeks post-implantation (D, E and F), the graft polymer is actively being absorbed in active islands of degradation and thin collagen bands are separating the islands of active absorption. At 52 weeks post-implantation (G, H and I) active islands of absorption remain, separated by broad bands of host connective tissue. Stains: A), D), and G) H&E = hematoxylin and eosin; B), E) and H), CD45 = leukocyte common antigen denoting inflammatory cells; and C), F), and I), MT = Masson trichrome stain = collagen green.

The in vivo remodeling of implanted grafts shows simultaneous and progressive resorption, replacement by collagenous host tissue, and decreasing inflammation (summarized in Fig. 11). The histological evaluation demonstrated that the evolving graft structure was spatially heterogeneous, with islands of resorbing polymer separated by bands of fibrous tissue. The luminal surface of the graft was covered with a well-organized, and apparently stable, neointima composed of collagen and partially lined by flattened cells that resembled endothelium. There was no evidence of calcification or infection in any grafts. Thus, the in vivo remodeling of the implanted graft shows resorption of polymer and progressive replacement by functional host tissue. These two phenomena happen simultaneously as evidenced by the semi-quantitative evaluation of component mechanical properties.

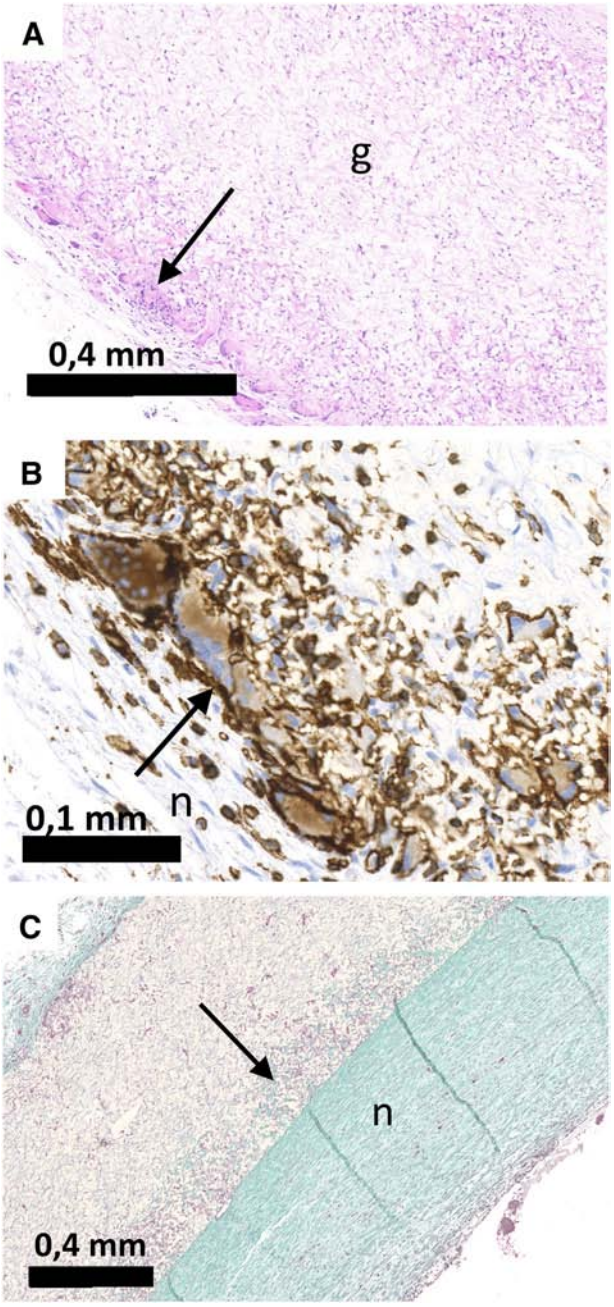


**Fig. 6.** Specific features of graft progression, at 8 weeks post-implantation. A) The graft (g) is largely intact and there is influx of inflammatory cells with graft absorption (arrow). B) Inflammatory cells with phagocytic activity and foreign body giant cells at the luminal surface of the polymeric graft below a thin neointima (n). The graft-neointima junction is marked by an arrow). C) There is early collagen formation within the graft (arrow). Stains: A) Hematoxylin and eosin; B) CD45 (leukocyte common antigen), denoting inflammatory cells; and C) Masson trichrome stain (collagen green).

The single graft related adverse event was an aneurysmal dilation in the mid-section of one graft (#4), detected at 8 weeks follow-up and confirmed at sacrifice at 10 weeks follow up. While it is impossible from the data available to ascertain the precise cause(s) and mechanisms for aneurysm formation in this sheep, analysis revealed that this was originally a false aneurysm (i.e., break in the wall permitting blood to extravasate outside of the vessel). Semi-quantitative histological assessment revealed more advanced absorption in this graft, which leads to the hypothesis that the implant may have focally lost its mechanical integrity before the new tissue achieved sufficient mechanical strength, potentially resulting from the local separation of the polymer

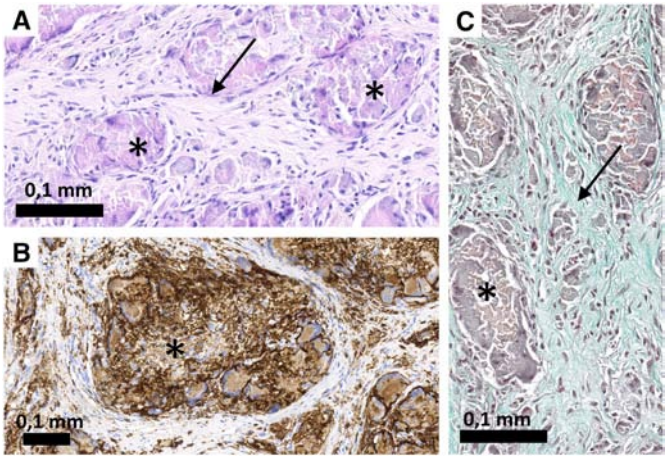


**Fig. 7.** Specific features of graft progression, 24 weeks post-implantation. A) The graft has been partially remodeled, with islands of resorbing polymer (asterisks) separated by thin bands of fibrous tissue (arrow). This is seen more clearly in B), which highlights brisk inflammatory cell activity in resorbing polymer islands (asterisk). C) Bands of cellular fibrous tissue (arrow) are evident between polymer islands (asterisk). Stains: A) hematoxylin and eosin; B) CD45 (leukocyte common antigen), denoting inflammatory cells; and C) Masson trichrome stain (collagen green).

into distinct islands by fibrous tissue ingrowth. Interestingly, this graft also showed the most advanced collagen deposition. We hypothesize that the region of advanced absorption triggered tissue formation in this specimen, but not fast enough to avoid dilation. Subsequently, collagen deposition stabilized the tissue, as the derived burst pressure for the dilated region was 1352 mmHg, and thereby higher than in the non-dilated section of the same graft (768 mmHg).

In an effort to understand the mechanism of advanced absorption of polymer in the specimen with a dilated segment, studies were done using an in vitro oxidation assay (solution containing 20% hydrogen peroxide and 0.1M cobalt(II) chloride) [20], the data indicated that the polymer batch used for this implant degraded atypically fast relative to other batches studied. Nevertheless, the same polymer batch was also used to fabricate the grafts in 3 other sheep (sacrificed at 11, 40 and 53 weeks, respectively) and none of these showed signs of aneurysms. Therefore, variation in batch properties are unlikely to be the only critical determinant of performance and other factors may have contributed. This finding highlights the importance of generating an appropriate balance between scaffold absorption and tissue formation globally and locally. Moreover, as there is a potential variability in both polymer absorption and tissue formation from individual to

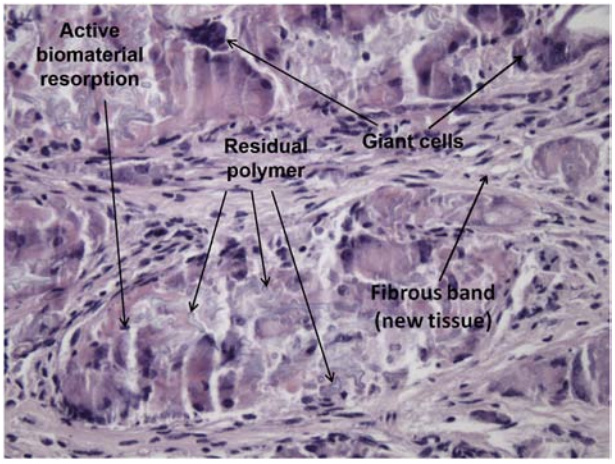


**Fig. 8.** High power photomicrograph of graft at 24 weeks reveals the active phagocytic process, yielding small polymer fragments, and foreign body giant cells, predominantly at the periphery of the islands of active degradation.

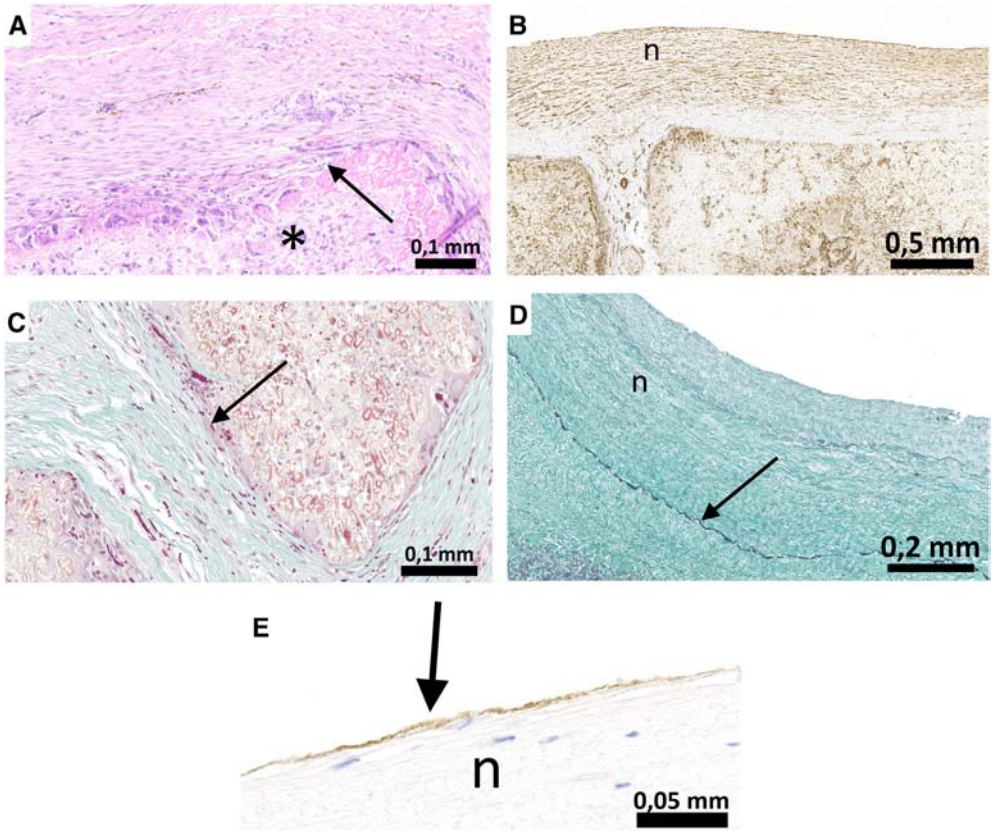


**Fig. 9.** Specific features of graft remodeling, 53 weeks post-implantation. A) Thick, dense collagen bands are present (arrow). Inflammatory cell infiltration and phagocytosis remain active within islands of polymer (asterisk). B) There is little inflammation outside of the resorbing polymer islands. Smooth muscle cells are prominent in the neointima (n). C) Broad collagen bands (arrow) are present. D) Elastin (arrow) is present at the junction of the neointima (n) with the graft. E) The neointima (n) is lined by endothelial cells (arrow). Stains: (A) hematoxylin and eosin; B) smooth muscle actin, denoting smooth muscle cells (C) Masson trichrome stain (collagen green D) von Giesen (elastin black); E) von Willebrand Factor, denoting endothelial cells.

individual, as a result of genetic differences, lifestyle factors, comorbid conditions, and local mechanical environment [21], it will be important to set-up rigorous specifications and standardized manufacturing procedures to ensure appropriate quality control on these specifications. This is most likely to ensure a consistent inherent degradation profile of the implant, to provide sufficient margin to accommodate unanticipated in vivo variability.

Our results reported herein extend previously published data that suggest that ETR, can replace a substrate polymeric graft solely by cells from the recipient, without the use of intentionally pre-seeded stem cells or animal-derived products [11,22–25]. The possibility of growth of the new tissue commensurate with somatic growth of a maturing recipient, although not demonstrated in this study, will be particularly important. This study provides further evidence that ETR might be a clinically feasible paradigm for a vascular graft and potentially other cardiovascular devices.

**Table 3**
Semi-quantitative analysis data for scaffold absorption and collagen deposition

| Ovine | Explantation time (weeks) | Collagen deposition score | Scaffold degradation score |
|---|---|---|---|
| #1 | 0 | N/A | N/A |
| #2 | 8 | 1 | 1 |
| #3 | 8 | 1 | 1 |
| #4 | 10 | 3 | 3 |
| #5 | 11 | 1 | 1 |
| #6 | 24 | 2 | 2 |
| #7 | 40 | 3 | 3 |
| #8 | 53 | 3 | 3 |
| #9 | 53 | 3 | 3 |

The proof of concept demonstrated by the animal results led to a feasibility (first in human) clinical trial involving 5 pediatric patients who underwent an extra-cardiac cavopulmonary connection procedure as part of a modified Fontan correction using the new vascular graft to connect the inferior vena cava to the right pulmonary artery [26]. No graft-related adverse events were detected during the clinical study up to 3 years follow up. Since many patients requiring right-sided reconstruction would benefit from a valved conduit, pre-clinical studies of a valved conduit were done [16]. Their favorable results justified a first-in human trial of 12 patients enrolled, each requiring right ventricular outflow reconstruction. In each case, the primary endpoint was met and there have been no reoperations or reinterventions up to 18 months. Detailed

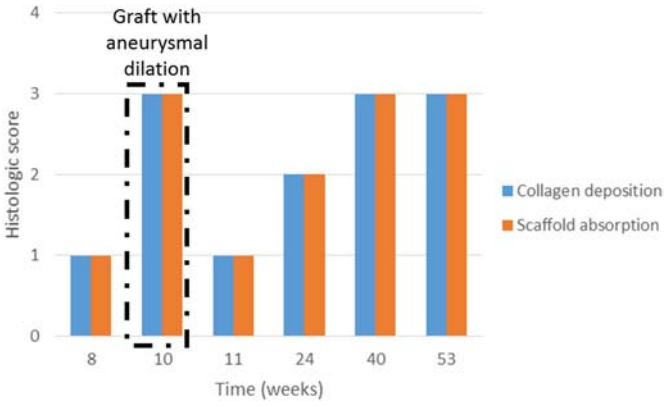


**Fig. 10.** Semi-quantitative histologic analysis of scaffold absorption and collagen deposition over time. Note that two animals are combined at 8 weeks and 53 weeks.

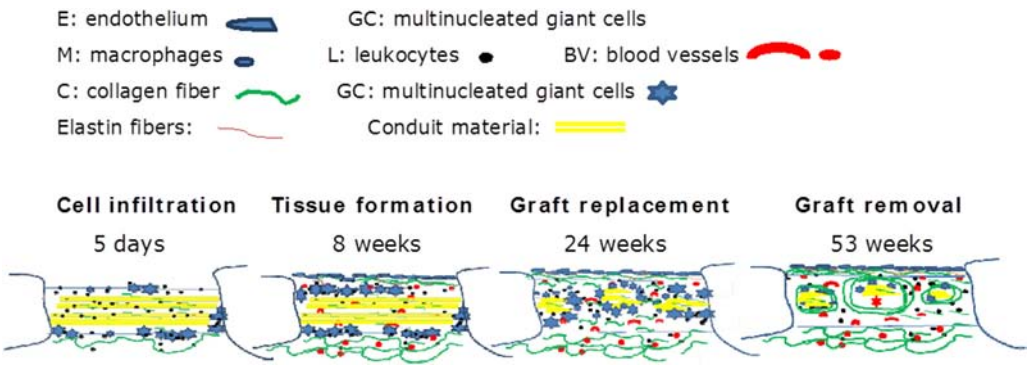


**Fig. 11.** Schematic representation summarizing key tissue events in pulmonary arterial conduits during ETR, adapted from Bockeria et al [26].

results of both clinical studies will be reported in subsequent publications.

## 5. Conclusion

Short to intermediate term implants in the pulmonary artery in adult sheep show that an off-the-shelf, electrospun, bioabsorbable polymeric vascular graft (without cell seeding prior to implantation) can undergo remodelling solely by recipient cells to create living tissues that can maintain function up to one year. Further pre-clinical and clinical investigation of the ETR concept is ongoing.

## References

[1] Costello JM, Pasquali SK, Jacobs JP, He X, Hill KD, Cooper DS, et al. Gestational age at birth and outcomes after neonatal cardiac surgery: An analysis of the Society of Thoracic Surgeons congenital heart surgery database. Circulation 2014;129:2511–7.
[2] Bobylev D, Breymann T, Boethig D, Haverich A, Ono M. Semilunar valve replacement with decellularized homograft after Damus-Kaye-stansel anastomosis and Fontan procedure. Ann Thorac Surg 2014;97:1792–5.
[3] Grubitzsch H, Laule M, Stangl K, Lembcke A, Sander M, Christ T, et al. Surgical transcatheter approach for endocarditis of a calcified aortic homograft. J Heart Valve Dis 2013;22:751–3.
[4] Lis GJ, Rokita E, Podolec P, Pfitzner R, Dziatkowiak A, Cichocki T. Mineralization and organic phase modifications as contributory factors of accelerated degeneration in homograft aortic valves. J Heart Valve Dis 2003;12:741–51.
[5] DiBardino DJ, Jacobs JP. Long-term management of patients undergoing successful pediatric cardiac surgery. Semin Thorac Cardiovasc Surg 2014;26:132–44.
[6] Vacanti JP, Morse MA, Saltzman WM, Domb AJ, Perez-Atayde A, Langer R. Selective cell transplantation using bioabsorbable artificial polymers as matrices. J Pediatr Surg 1988;23:3–9.
[7] Niklason LE, Gao J, Abbott WM, Hirschi KK, Houser S, Marini R, et al. Functional arteries grown in vitro. Science 1999;284:489–93.
[8] L'Heureux N, Dusserre N, Konig G, Victor B, Keire P, Wight TN, et al. Human tissue engineered blood vessel for adult arterial revascularization. Nat Med 2006;12:361–5.
[9] Hoerstrup SP, Cummings I, Lachat M, Schoen FJ, Jenni R, et al. Functional growth in tissue-engineered living, vascular grafts: Follow-up at 100 weeks in a large animal model. Circulation 2006;114:I-159–66.
[10] Shin'oka T, Matsumura G, Hibino N, Naito Y, Watanabe M, Konuma T, et al. Midterm clinical result of tissue-engineered vascular autografts seeded with autologous bone marrow cells. J Thorac Cardiovasc Surg 2005;129:1330–8.
[11] Talacua H, Smits AIPM, Muylaert DEP, van Rijswijk JW, Vink A, Verhaar MC, et al. In situ tissue engineering of functional small-diameter blood vessels by host circulating cells only. Tissue Eng 2015;21:2583–94.
[12] Syedain Z, Reimer J, Lahti M, Berry J, Johnson S, Bianco R, et al. Tissue engineering of acellular vascular grafts capable of somatic growth in young lambs. Nat Commun 2016;7:12951.
[13] Kluin J, Talacua H, Smits AI, Emmert MY, Brugmans MC, Floretta ES, et al. In situ heart valve tissue engineering using a bioresorbable elastomeric implant – From material design to 12 months follow-up in sheep. Biomaterials 2017;125:101–17.
[14] Wissing TB, Bonito V, Bouten CVC, Smits AIPM. Biomaterial-driven in situ cardiovascular tissue engineering-a multi-disciplinary perspective. NPJ Regen Med 2017;2:18. https://doi.org/10.1038/s41536-017-0023-2.
[15] Bouten CVC, Smits AIPM, Baaijens FPT. Can we grow valves inside the heart? Perspective on material-based in situ heart valve tissue engineering. Front Cardiovasc Med 2018;5:54. https://doi.org/10.3389/fcvm.2018.00054.
[16] Bennink G, Torii S, Brugmans M, Cox M, Svanidze O, Ladich E, et al. A novel restorative pulmonary valved conduit in a chronic sheep model: Mid-term hemodynamic function and histologic assessment. J Thorac Cardiovasc Surg 2018;155:2591–601.
[17] Sijbesma RP, Beijer FH, Brunsveld L, Folmer BJ, Hirschberg JH, Lange RF, et al. Reversible polymers formed from self-complementary monomers using quadruple hydrogen bonding. Science 1997;278:1601–4.
[18] Bosman AW, Sijbesma RP, Meijer EW. Supramolecular polymers at work. Mater Today 2004;7:34–9.
[19] Lam CX, Hutmacher DW, Schantz JT, Woodruff MA, Teoh SH. Evaluation of polycaprolactone scaffold degradation for 6 months in vitro and in vivo. J Biomed Mater Res A 2009;90:906–19.
[20] Brugmans MCP, Söntjens SHM, Cox MAJ, Nandakumar A, Bosman AW, Mes T, et al. Hydrolytic and oxidative degradation of electrospun supramolecular biomaterials: In vitro degradation pathways. Acta Biomater 2015;27:21–31.
[21] Avishai E, Yeghiazaryan K, Golubnitschaja O. Impaired wound healing: facts and hypotheses for multi-professional considerations in predictive, preventive and personalised medicine. EPMA J 2017;8:23–33.
[22] Wu W, Allen RA, Wang Y. Fast-degrading elastomer enables rapid remodeling of a cell-free synthetic graft into a neoartery. Nat Med 2012;18:1148–53.
[23] De Valence S, Tille J-C, Mugnai D, Mrowczynski W, Gurny R, Moller M, et al. Long term performance of polycaprolactone vascular grafts in a rat abdominal aorta replacement model. Biomaterials 2012;33:38–47.
[24] Mrowczynski W, Mugnai D, de Valence S, Tille J-C, Khabiri E, Cikirikcioglu M, et al. Porcine carotid artery replacement with biodegradable electrospun poly-e-caprolactone vascular prostheses. J Vasc Surg 2014;59:210–9.
[25] Chen F-M, Wu L-A, Zhang M, Zhang R, Sun H-H. Homing of endogenous stem/progenitor cells for in situ tissue regeneration: Promises, strategies, and translational perspectives. Biomaterials 2011;32:3189–209.
[26] Bockeria L, Svanidze O, Kim A, Shatalov K, Makarenko V, Cox MAJ, et al. Total cavopulmonary connection with a new bioabsorbable vascular graft: First clinical experience. J Thorac Cardiovasc Surg 2017;153:1542–50.